Available online at www.sciencedirect.com
SCIENCE DIRECT®
Surface Science 530 (2003) 71–86
SURFACE SCIENCE
www.elsevier.com/locate/susc

Site preference of CO chemisorbed on Pt(1 1 1) from density functional calculations

Alfred Gil [a], Anna Clotet [a], Josep M. Ricart [a,*], Georg Kresse [b], Maite García-Hernández [c], Notker Rösch [c], Philippe Sautet [d,e,*]

[a] *Departament de Química Física i Inorgànica, Universitat Rovira i Virgili, Pl. Imperial Tàrraco 1, E-43005 Tarragona, Spain*
[b] *Institut für Materialphysik and Center for Computational Materials Science, Universität Wien, Sensengasse 8/12, A-1090 Wien, Austria*
[c] *Institut für Physikalische und Theoretische Chemie, Technische Universität München, 85747 Garching, Germany*
[d] *Institut de Recherches sur la Catalyse, Centre National de la Recherche Scientifique, 2 Avenue Albert Einstein, Villeurbanne Cedex 69626, France*
[e] *Laboratoire de Chimie Théorique, Ecole Normale Supérieure de Lyon, 46 Allée d'Italie, Lyon 69364, Cedex 07, France*

Received 15 October 2002; accepted for publication 28 January 2003

Abstract

Chemisorption of carbon monoxide on monocoordinated and tricoordinated sites of Pt(1 1 1) is studied using various computational methods based on density functional theory and a series of cluster and periodic models. Calculated results for geometries and binding energies are provided. We demonstrate that both types of models, irrespective of the density functional approximation used, always favour CO adsorption at the threefold coordinated hollow site instead of on-top, monocoordinated CO, as already suggested in the paper of Feibelman et al. [J. Phys. Chem. B 105 (2001) 4018]. This is at variance with experimental evidence and indicates a possible limitation of common approximate density functional theory methods. It is shown that small clusters, that do not correctly describe the substrate environment of the active site, are not adequate models to obtain adsorption energies or adsorption energy differences. However, with increasing cluster size, cluster results are very close to results of periodic calculations. The new insight is that hybrid functionals including a part of the exact exchange decrease the energy difference between the two positions, suggesting a stabilization of the on top site relative to the threefold hollow site in the limit of extended models. Arguments are presented that the energetic preference of the threefold hollow site is due to an inadequate description of the HOMO–LUMO gap.

Keywords: Density functional calculations; Chemisorption; Carbon monoxide; Platinum; Clusters

1. Introduction

The chemisorption of carbon monoxide (CO) on metallic surfaces has received great attention in the past decades. One of the reasons for this interest is that CO adsorption is a crucial step for several catalytic reactions such as CO oxidation, CO

* Corresponding authors.
E-mail addresses: ricart@quimica.urv.es (J.M. Ricart), sautet@chimie.ens-lyon.fr (P. Sautet).

0039-6028/03/$ - see front matter © 2003 Elsevier Science B.V. All rights reserved.
doi:10.1016/S0039-6028(03)00307-8

hydrogenation, or Fischer–Tropsch reaction, among others [1,2]. Moreover, due to its simplicity and well known adsorption properties, CO is generally used as a probe molecule in surface science. Its interaction with platinum surfaces is of great interest because of technological applications as catalyst in car exhausts, to promote the oxidation of CO to CO_2. A large number of studies, both experimental [3–14] and theoretical [15–23], focused on this chemisorption system analysing different surface planes, especially those of low Miller indices.

The theoretical description of the chemisorption of CO on Pt(1 1 1) has been the subject of a recent comprehensive study by Feibelman et al. [24]. This system was clearly pointed out as a challenge for theorists because all calculations based on periodic models and gradient-corrected GGA density functional theory (DFT) were shown to give an incorrect description of the CO adsorption site, when all computational parameters are well converged. Although no cluster calculation was performed in that study, it was suggested that well converged cluster calculations should give similar results to periodic models. The purpose of the present paper is to explore the relation between cluster and periodic models and to assess the importance of exact exchange in a hybrid exchange-correlation (xc) functional for the description of the CO-surface bonding. We will first briefly recall the experimental and theoretical background for this problem, and the reader can refer to Ref. [24] for a more thorough and complete presentation.

On the close packed Pt(1 1 1) surface, CO can form several structures as a function of the coverage θ_{CO} the main ones being a $(\sqrt{3} \times \sqrt{3})$-R30° structure at a third of a monolayer (ML), $\theta_{CO} = 1/3$ ML, and a c(4 × 2) structure at $\theta_{CO} = 1/4$ ML. Previous EELS studies [25–27] proposed that the observed CO stretching frequency corresponds to an initial occupation of on top sites at $\theta_{CO} = 1/3$ ML, which at a higher coverage ($\theta_{CO} = 1/2$ ML) evolves into a mixed occupation of on top and bridge sites. These vibrational assignments of the sites were later confirmed by dynamic LEED studies [14,28]. Real space images of CO chemisorption obtained with a scanning tunnelling microscope (STM) technique showed that at low coverage two sites are occupied by CO molecules [29–31]. From a comparison with simulated STM images, these sites were attributed to on top and bridge sites [32]. For the half monolayer case, only the structure with half of the CO molecules at on top sites and the other half in bridge sites yields simulated STM images that correspond to those found experimentally [31]. Hence, the general trend derived from these assignments is that CO on Pt(1 1 1) adsorbs preferentially at low coordinated on top sites, and at high coverage in association with bridge sites.

A large variety of theoretical methods was used to study the chemisorption of CO on Pt(1 1 1). Initial work was performed with semiempirical approximations [33–37], but in more recent calculations the interaction between the molecule and the surface was described with first principles methods, without adjustable parameters. Nowadays, methods based on DFT are routinely applied to this kind of systems, because the Kohn–Sham approach affords an efficient treatment of electronic correlation, with a similar computational cost as the Hartree–Fock (HF) method. The reliability of the DFT approach depends on the approximation of the xc functional. Recent studies usually go beyond the well known local density approximation (LDA) and are based on the generalized gradient approximation (GGA) or on hybrid functionals such as B3LYP, where an exchange contribution of a single-determinant configuration (similarly to Hartree–Fock) is included in the xc functional. Besides these quantum chemical approaches, the system CO/Pt(1 1 1) has also been studied with Monte Carlo [38] and molecular dynamics simulations [39].

In the framework of ab initio calculations there are two major strategies to model a surface, the periodic supercell and the cluster approaches. In the cluster approach, an adsorption site is modeled with a few atoms, which, thanks to modern technology, can include up to a few tens of atoms. One of the weaknesses of this methodology is that the calculated adsorption energies are rather dependent on the cluster size, a consequence of the fact that the description of the band structure of the metal is rather limited in this approximation. Nevertheless, local properties such as geometries

or frequencies are quite well described. In contrast, the supercell approach employs periodic slabs and exploits the translational symmetry of the system. Such periodic calculations avoid problems related to the artificial cluster boundaries, once the limitations associated with the finite number of layers of the model are under control. However, very recently, nanoparticle models, bound by low-index crystal planes, were shown to yield also accurate estimates of chemisorption energies for cluster models of about 80–150 transition metal atoms [40]. Another advantage of supercell models is connected to the fact that they are well suited for studying different coverages of adsorbates on the surface. Moreover, describing the surface by a periodic system enables to use a plane wave basis set to describe one-electron wavefunctions, hence avoiding the problem of basis set choice. Unfortunately, hybrid functionals are not available with current plane wave codes. Although (approximate) DFT-based methods are reasonably accurate, it is not clear whether they can provide a reliable way to simulate and interpret surface chemical problems, where energies of different sites usually differ by only a few tenths of an electron volt (eV). Such a small energy difference can rationalize the experimentally observed additional occupation of bridge sites, besides the top sites expected in the low coverage regime.

A compilation of the results obtained so far from ab initio calculations for the CO–Pt adsorption system shows an interesting feature. The two different model strategies mentioned above apparently yield results at variance with experiment for the preferred chemisorption site of CO in the low coverage regime. Several papers devoted to the adsorption of CO on Pt(1 1 1) use the periodic approach. With the exception of the earlier work of Philipsen et al. [22], the top site was found to be less favourable than the hollow site. However, in Ref. [22] only two metal layers were considered and the CO distance was not optimised. Lynch and Hu [18] used the GGA approximation of Perdew and Wang [41,42], to study an extended slab containing three layers of Pt atoms, the first of which was allowed to relax, with CO placed in a $p(2 \times 2)$ supercell. They reported binding energies of 2.00, 2.09 and 1.87 eV for CO adsorbed on fcc, hcp and on top sites, respectively. Feibelman et al. [24], in the previously mentioned comprehensive paper, explored several supercells and coverages of CO over the Pt surface, using purely semilocal functionals and three different codes. They found that adsorption in fcc sites is more stable than at on top sites in all cases, with energy differences ranging from 0.10 to 0.45 eV. Finally, in a very recent paper, Grinberg et al. [43] analyzing the same puzzling system, concluded that converged pseudopotentials and all-electron calculations yield very similar results and that the binding energy at the hollow site is overestimated (entailing the major modeling error for this adsorption system), while the top site is treated accurately, thus arguing that the error due to the GGA depends on the local coordination of CO. All the results disagree with experimental findings; thus, the question arises whether important electronic aspects are correctly described by DFT-GGA xc functionals.

On the other hand, several results obtained from cluster models of the Pt(1 1 1) surface are available. In order to compare them more easily, we classified the clusters according to the number of first neighbors added to the atoms that form a given adsorption site. The clusters are noted as (n, p) where n and p are the number of metal atom neighbors (of the site atoms) in the first and second layers, respectively. For the on top adsorption site, results for (6,3) models were reported. Liao et al. [44] obtained an adsorption energy of 1.16 eV using a GGA functional (VWN-BP) [45–47]. Wasilesky et al. [48] calculated an adsorption energy of 1.26 eV with the BP86 functional. Curulla et al. [17] used the B3LYP hybrid functional and calculated an adsorption energy of 1.14 eV. The same work reports a binding energy of 2.37 eV using B3LYP and (0,3) models, in agreement with Illas et al. [49]. The initial adsorption energy for CO bonded on top at a Pt(1 1 1) surface was measured at about 1.4 eV [50–52], a value which is close to the theoretical results obtained with the higher quality (6,3) models. This fact points to the need for a good description in terms of surrounding atoms of the adsorption site, to obtain a reliable value of the binding energy for a given system. To the best of our knowledge, there is no data in the

literature related to the study of CO adsorption in a hollow site on Pt(1 1 1) with models of (6,3) quality or better. The best description found, with clusters of (4,3) quality, was performed by Wasilesky et al. [48], who reported an adsorption energy of 1.28 eV.

Hence, at variance with slab model results, cluster calculations [17,49,53] seem to favour the on top site, in agreement with experimental data; the only exception is the study of Wasilesky et al. [48] which yielded essentially degenerate sites, slightly favouring the hollow site by 0.02 eV. However, only small clusters have been used. Therefore, the origin of the difference between cluster and slab calculations cannot be uniquely determined, because both calculations were performed under different conditions and several factors may contribute to such a discrepancy. Different cluster sizes and shapes were used, and artefacts from finite cluster size could play an important role. Apart from the model, the calculations differed in technical aspects, such as the choice of xc functional or effective core potentials.

The goal of the present work is to identify the origin of the difference between periodic and cluster approach results, by performing a study of CO chemisorption using slab and cluster models where one tries to minimize the differences between the two approaches. This will give a clue as to which factors are important for achieving a reliable computational description of CO chemisorption on Pt(1 1 1) in particular and of surface chemistry in general.

2. Models and computational details

2.1. Cluster model

To compare periodic plane wave and cluster calculations, the Pt(1 1 1) surface was represented by a cluster of 18 Pt atoms (Fig. 1). It is built up starting with three nearest-neighbor atoms, which simulate the face centered cubic (fcc) threefold hollow site. The first neighbors of those atoms were added both in the first and in the second layer. With this model, we have a good description of the coordination of the Pt atoms involved in the chemisorption site, both for the fcc hollow (F in Fig. 1a) and on top (T in Fig. 1a) cases. In fact, showing a better description of the adsorption sites, this model is an improvement with respect to others found in the literature. The use of the same cluster model to study different sites permits to compare directly the calculated properties without worrying about changes associated with different cluster models. The positions of the atoms have been fixed as in bulk platinum, with the experimental lattice parameter of 3.924 Å, yielding a Pt–Pt distance of 2.775 Å. Calculations were performed using both the gradient-corrected GGA xc functional PW91 [42] and the hybrid functional B3LYP [54], as implemented in the Gaussian 98 suite of programs [55]. For the Pt_{18} cluster, the $5s^25p^65d^96s^1$ electrons of every platinum atom were explicitly considered within the LANL2DZ basis set, whereas the inner core was described by means of a relativistic effective small core pseudopotential (ECP) as proposed by Hay and Wadt [56]. For CO, all electrons were explicitly considered, and three different standard basis set were used, to analyse the basis set effect. We first

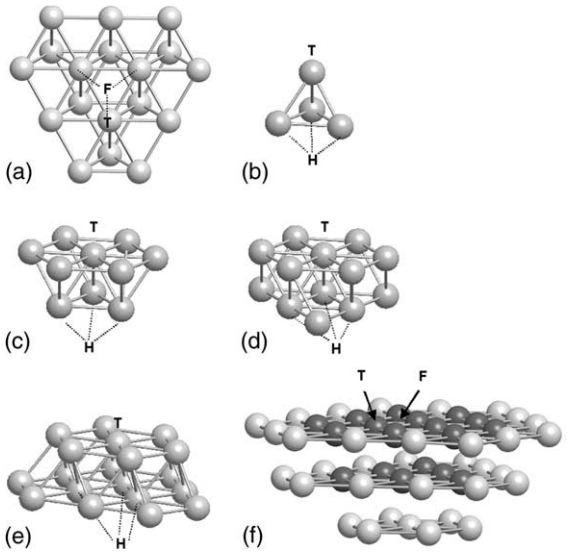

Fig. 1. Cluster models employed in this study: (a) top view of the cluster Pt_{18}, marks indicate fcc (F) and on top (T) sites; (b) Pt_4; (c) Pt_{10}; (d) Pt_{13}; (e) Pt_{19}; (f) Pt_{52} cluster, constructed by adding all first neighbors to the cluster Pt_{18} (darker atoms). In panel (f), bonds between layers are suppressed for clarity.

used a double-ζ basis set, 6-31G* and improved the quality by switching to a triple-ζ basis set, 6-311G*; finally we added diffuse functions to reach the 6-311G* + basis set. Geometry optimisations were performed with the Berny algorithm using internal coordinates. Adsorption energies were calculated as the difference between the total energy for the optimised system (adsorption system) and the sum of total energies of its fragments (non-adsorbed system), optimised with the same basis set. Binding energies were always corrected for the basis set superposition error (BSSE), using the counterpoise method proposed by Boys and Bernardi [57].

A series of small to medium-size cluster models, Pt_4, Pt_{10}, Pt_{13} and Pt_{19} was also considered, see Fig. 1b–e. These clusters permit to study both on top and hcp hollow sites (labelled T and H, respectively in Fig. 1b–e), just by changing the side of the cluster on which the CO molecule adsorbs. In this series of clusters, the hollow site is hcp, at variance with other models used here (Pt_{18}, Pt_{52} and slabs, see below), where this site is fcc. This election was done to fully exploit the cluster symmetry, but does not affect the conclusion that the hollow site is always preferred, as will be shown below.

The cluster calculations were performed with three codes. As indicated, we used Gaussian98 for Pt_{18}. For the cluster series just mentioned, we employed the LCGTO-FF-DF method (linear combination of Gaussian type orbitals fitting function density functional) [58] as implemented in the parallel code PARAGAUSS [59,60], where large and flexible all-electron Gaussian type basis sets are used for expanding the Kohn–Sham orbitals. For Pt atoms we used a (21s, 17p, 12d, 7f) basis set, contracted to [10s, 8p, 5d, 3f] [61]. For C and O atoms we selected a (9s, 5p, 1d) contracted to [5s, 4p, 1d] [62]. Scalar relativistic effects were included by means of the Douglas–Kroll–Hess approach to the Dirac–Kohn–Sham problem [63]. Geometries were optimised at the LDA that yields good results for bond distances; we used the parameterisation suggested by Vosko, Wilk and Nusair (VWN) [46]. For these geometries, we calculated the energies using two gradient-corrected GGA xc functionals: the one proposed by Becke and Perdew (BP) [45] and a revised version of the Perdew–Burke–Ernzerhoff functional (rPBE) [64]. To reach convergence during the SCF procedure, we used a fractional occupation number technique with a very small level broadening of 0.01 eV [58]. Results were also corrected for BSSE. The third approach with which clusters were calculated corresponds to the periodic approach described in the following section.

2.2. Slab model

The Pt(1 1 1) surface was modeled by a periodic four-layer Pt slab with a CO adlayer adsorbed on one side of the slab. Most of the calculations were made with a $(\sqrt{3}\times\sqrt{3})$-R30° structure ($\theta_{CO} = 1/3$ ML) (Fig. 2). For better comparison with the cluster results, a larger (3×3) cell was also computed, corresponding to the low coverage regime ($\theta_{CO} = 1/9$ ML). Each slab is separated from its periodic image in the z-direction by a vacuum space equivalent to six missing metallic layers, to avoid interactions between slabs. The positions of the Pt atoms were frozen as in the bulk metal with experimental lattice parameters, like in cluster calculations, although tests were made to check the effect of an optimised bulk lattice parameter and of the relaxation of the two uppermost layers on the energy. This choice of the experimental lattice constant, instead of the commonly used optimised value for the bulk, was done for consistency with the cluster calculations. It explains some small deviations of the results compared to other published periodic calculations. It has,

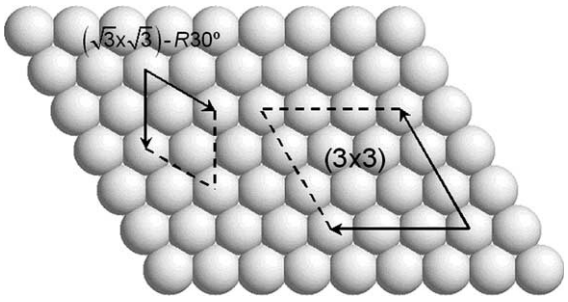

Fig. 2. Slab model top view. Two of the studied supercells are shown: $(\sqrt{3}\times\sqrt{3})$-R30° structure corresponds to $\theta_{CO} = 0.33$ ML; (3×3) structure corresponds to $\theta_{CO} = 0.11$ ML.

however, no significant effect on the difference in binding energy between top and hollow site. Calculations were performed using the Vienna Ab-initio Simulation Package (VASP) [65–67]. The xc functional was the gradient-corrected form proposed by Perdew and Wang (PW91) [42]. The electron–ion interaction was described by means of the projector augmented wave (PAW) approach [68] and the cutoff energy was set to 500 eV. Brillouin zone integrations were performed on a $9 \times 9 \times 1$ grid of Monkhorst–Pack points [69].

In addition to these slab model calculations, spin restricted VASP calculations were performed for all clusters considered before to compare cluster with periodic models in as closely a fashion as possible and clusters described by local basis or plane waves. It should be noted, however, that VASP applies fractional occupation numbers in a similar manner as PARAGAUSS [58] to improve the convergence of the SCF process. The present results were always extrapolated to zero smearing.

The clusters were positioned in a large cubic cell, yielding a closest distance of 7 Å between Pt atoms in different periodic images. Tests with a larger separation between clusters (9 Å) yielded essentially the same results. Furthermore, a Pt_{52} cluster was also studied, in order to investigate the influence of cluster size effects. That cluster was constructed by adding a shell of second neighbors to the Pt_{18} cluster (Fig. 1f). The Pt_{52} cluster comprises 27 atoms in the "top" crystal plane, 18 atoms in the second plane, and 7 atoms in the third plane.

3. Results and discussion

3.1. Cluster calculations

The adsorption of CO on Pt(1 1 1) was first studied with the Pt_{18} cluster model (Fig. 1a). The size of this cluster is such that all the metal atoms interacting with the CO adsorbate have complete shells of nearest neighbor atoms, both for the top and hollow adsorption sites. As stated above, the calculations were performed with two approaches: either with atomic orbitals or plane waves as basis set, and with different xc functionals. The B3LYP calculations could only be realized with a localized Gaussian type orbital (GTO) basis set. The results, collected in Table 1, give a very similar binding

Table 1
Calculated structural and energetic properties of CO adsorbed on top and at fcc sites of Pt(1 1 1) represented by the Pt_{18} and Pt_{52} cluster models using different xc functionals and basis sets (Gaussian-type orbitals—GTO, plane wave—PW)

Cluster	Functional	Basis set	Site	d_{C-S} (Å)	d_{C-O} (Å)	BE (eV)	ΔE (eV)
Pt_{18}	B3LYP	GTO-dζ	top	1.866	1.149	1.42	−0.04
			fcc	1.375	1.185	1.46	
	B3LYP	GTO-tζ	top	1.865	1.139	1.40	−0.05
			fcc	1.373	1.176	1.45	
	B3LYP	GTO-tζ+	top	1.865	1.139	1.42	−0.07
			fcc	1.369	1.176	1.49	
	PW91-HF[a]	GTO-dζ	top	1.856	1.160	1.91	−0.31
			fcc	1.378	1.197	2.22	
	PW91	PW (7 Å)	top	1.860	1.157	1.68	−0.35
			fcc	1.363	1.195	2.03	
	PW91	PW (9 Å)	top	1.861	1.157	1.69	−0.34
			fcc	1.363	1.196	2.03	
	BP86	PW (7 Å)	top	1.867	1.157	1.55	−0.30
			fcc	1.365	1.194	1.85	
Pt_{52}	PW91	PW (7 Å)	top	1.879	1.156	1.32	−0.14
			fcc	1.394	1.193	1.46	

GTO results obtained with Gaussian98 (dζ, tζ, and tζ+ account for double, triple and triple plus polarization basis sets for CO). PW results with VASP (in parenthesis, distance between two clusters). d_{C-S} is the distance along the surface normal from C to the top layer, and d_{C-O} the C–O bond length. ΔE (eV) is the difference between top and fcc site; negative if the fcc site is more stable.

[a] Perdew–Wang functional with a 1% exact exchange, see text.

energy for the top and fcc hollow site. The hollow site is found to be slightly more stable than the on top site by 0.04–0.07 eV, depending on the selected basis set. The choice of a triple-ζ basis set (t-ζ) or the addition of a diffuse function (t-ζ+) has, in fact, only a small influence on the calculated binding energy and geometry. The double-ζ basis set is hence already satisfactory.

Within this GTO approach, the obtained PW91 result is significantly different from the B3LYP one. In a first step, calculations on this system with the PW91 functional were not successful, because Gaussian98 did not find the correct ground state. It is well known that local density and GGA xc functionals have the tendency to give small HOMO–LUMO gaps, and convergence problems are common. Several conventional procedures implemented in the code to aid convergence were tested, but they all failed. Then a new strategy was started, and the cluster calculation was performed with a "user-made" hybrid functional, which includes only 1% of exact exchange, instead of 20% as in the B3LYP parameterisation. Addition of such a small amount of exact exchange helps to open the gap between the HOMO and the LUMO and allows to reach convergence, while this xc approximation is almost of the GGA form. With this PW91-like functional, the CO adsorption energy is strongly increased, especially for the hollow site (0.76 eV), and the CO bond is slightly elongated. Adsorption on the hollow fcc sites is favoured by 0.31 eV compared to on top adsorption.

These cluster results for the PW91 xc functional, obtained with a localized basis set, are reproduced in the cluster calculation using a plane wave basis. In the latter case, the hollow site is favoured by 0.35 eV, and the calculated distances are very similar to those computed in the GTO approach. The only significant difference is a slightly reduced adsorption energy for both sites. A larger cell in which the cluster is contained does not lead to significant changes; also, changing to a different GGA functional (BP86) does not have a significant influence, neither on the geometry nor on the difference in binding energy between the sites. Only the binding energy for each adsorption site decreases slightly. Therefore, on the Pt_{18} cluster, results from purely semilocal GGA and hybrid B3LYP calculations, favouring adsorption on the hollow site, are both at variance with experiment. However, the energy difference between sites is smaller with B3LYP. For this hybrid DFT approach, the values of the binding energy compare much better with experiment (1.43 eV) [3], while PW91 seems to overestimate it. The latter result is in line with findings for metal–ligand binding energies [70,71]. At this point, however, artefacts from the finite cluster model cannot be determined. For the top site, all calculated C–O and C–S (distance along the surface normal from C to the top layer) distances compare well with the LEED results [14,28] (1.15 and 1.85 Å respectively), although the CO distance is slightly longer for GGA functionals.

With the periodic plane wave approach, it was possible to consider a larger Pt_{52} cluster where artefacts from the finite size of the cluster should be much reduced. Compared to the case of Pt_{18} in the same calculation conditions, the adsorption energy on the Pt_{52} cluster is significantly reduced, especially in the case of the hollow site. As a result, the energy difference between sites in Pt_{52} is half the value calculated for Pt_{18} however still with the incorrect sign. The C–S distance is slightly elongated but the C–O distance does not change.

The calculations performed with the Pt_{18} and Pt_{52} clusters cannot be compared with the previous cluster calculations found in the literature because there smaller model clusters have been used. Therefore a series of smaller cluster models, Pt_4, Pt_{10}, and Pt_{13} was studied. (The series is completed by the Pt_{19} cluster, where coordination of the on top and threefold sites was similar to that provided by the Pt_{18} cluster, but with a threefold hcp site instead of an fcc one.) First, parallel calculations to the ones performed on Pt_{18} were completed: B3LYP functional with a localized basis set and PW91 functional with a plane wave basis set. Furthermore, an all-electron localized orbital approach was used as well, employing different GGA functionals (see above).

The adsorption energy was calculated to decrease in the order PW91, BP, rPBE, B3LYP. That behaviour is the expected one for the purely semilocal functionals, as shown in several examples of chemisorption systems [64], the hybrid

functional not being included in that study. If we just consider the energy difference between the two sites, the same order is observed for the xc functionals, PW91 showing the highest energy difference favouring three-coordinated adsorption sites, and B3LYP showing the smallest difference. Nevertheless, the differences given by the pure functionals are very similar, except for the smallest Pt_4 cluster, although the cluster is too small to model the surface properly.

The most important effect observed in Table 2 is the strong cluster size dependence. In comparison with the previous Pt_{18} data, the smaller Pt_4 model yields too short vertical distances to the surface, C–S, for both sites and all considered approaches and slightly longer C–O distances. The underestimation of C–S distances is particularly severe in the case of the hcp hollow site, where changes are of the order of 10%. For the top site and larger clusters, the discrepancies are generally smaller. For the Pt_{10} and Pt_{13} cluster, the C–O distances do not differ from that of Pt_{18}, and C–S distances are within a 0.3% for the on top site and 3–4% for the hcp site. Obviously, the energy difference between the two adsorption sites is not properly described with the small models Pt_4 and Pt_{10}. In Pt_{10}, this difference is much too large. On the other hand, for Pt_{13} the energy difference is quite similar to the

Table 2
Calculated structural and energetic properties for CO adsorbed on Pt(1 1 1) represented by the Pt_4, Pt_{10}, Pt_{13} and Pt_{19} cluster models

Cluster	Functional	Site	d_{C-S} (Å)	d_{C-O} (Å)	BE (eV)	ΔE (eV)
Pt_4	B3LYP	top	1.851	1.157	1.26	0.13
		hcp	1.218	1.208	1.13	
	PG-BP86	top	1.816	1.156	2.68	0.06
		hcp	1.160	1.215	2.63	
	PG-rPBE	top	1.816	1.156	2.37	0.11
		hcp	1.160	1.215	2.26	
	PW-PW91	top	1.856	1.165	2.63	−0.06
		hcp	1.217	1.220	2.69	
Pt_{10}	B3LYP	top	1.860	1.149	1.21	−0.66
		hcp	1.417	1.185	1.87	
	PG-BP86	top	1.826	1.148	1.77	−0.84
		hcp	1.303	1.197	2.60	
	PG-rPBE	top	1.826	1.148	1.45	−0.81
		hcp	1.303	1.197	2.26	
	PW-PW91	top	1.862	1.157	1.78	−0.85
		hcp	1.360	1.202	2.63	
Pt_{13}	B3LYP	top	1.872	1.148	1.18	−0.12
		hcp	1.428	1.183	1.30	
	PG-BP86	top	1.821	1.148	1.76	−0.24
		hcp	1.291	1.196	2.00	
	PG-rPBE	top	1.821	1.148	1.31	−0.21
		hcp	1.291	1.196	1.52	
	PW-PW91	top	1.860	1.158	1.76	−0.31
		hcp	1.362	1.199	2.07	
Pt_{19}	PG-BP86	top	1.823	1.148	1.34	−0.14
		hcp	1.321	1.190	1.48	
	PG-rPBE	top	1.823	1.148	1.13	−0.11
		hcp	1.321	1.190	1.24	
	PW-PW91	top	1.860	1.158	1.49	−0.29
		hcp	1.378	1.194	1.78	

Three codes were used, two employing GTO orbitals and one a plane wave expansions. GTO: pseudopotential Gaussian98 (G98/ECP) with B3LYP (double-ζ plus polarization basis set for CO); PG-PB86 and PG-RPBE: all-electron PARAGAUSS (PG/AE) with VWN geometries and BP86 and rPBE energies; PW-PW91: VASP with PW91 functional. See Table 1 for the definition of the specified values.

values obtained for the larger Pt_{18} cluster, in particular in the case of the plane wave calculation. For these smaller clusters, the all-electron approach yields weaker binding energies than the plane wave method, but not as weak as the energies obtained with the hybrid pseudopotential approach. Energy differences between both sites are larger than those for the B3LYP method, but still smaller than the plane wave PW91 values.

In general, the results for Pt_{13} do not differ much from those reported for Pt_{18}: all models favour hollow site adsorption, B3LYP results produce smaller energy differences. On the other hand, Pt_{10} results are notably modified, with large energy differences because the hollow site is calculated too stable, by 0.6 eV, for all cases. Apparently, the top site is reasonably described in this cluster (six nearest-neighbors in the first layer, three in the second layer), but in the case of hcp site, the environment of the surface Pt atoms interacting with the CO is not correctly modeled. The atoms describing an hcp site should be surrounded by nine atoms in the first layer and seven in the second, and in the Pt_{10} cluster only the atoms in the second layer are present. For Pt_{19}, computed by the all-electron localized orbitals approach, the absolute stability of both adsorption sites decreases compared to the smaller clusters; although the hollow site is still preferred. The difference of the energies also decreases, to 0.14 and 0.11 eV for BP86 and rPBE xc functionals, respectively.

In conclusion, small clusters, that do not correctly describe the substrate environment of all surface sites under consideration, are not adequate models for the description of adsorption energies or adsorption energy differences. However, some strategies such as the use of the bond preparation [72,73] have been successful in obtaining adequate binding energies.

3.2. Periodic calculations

The trend observed with the large cluster Pt_{52} is confirmed by the results obtained from periodic calculations. This approach provides all surface atoms involved in the adsorption process with their correct environment. The present slab calculations address different CO coverages with varying numbers of layers in the slab model, and different GGA xc functionals. Comparison of on top and fcc adsorption shows that the fcc hollow site is preferred by CO (Table 3), in agreement with previous plane wave studies [18,24]. The energy difference between fcc and on top sites ranges from 0.11 to 0.15 eV. These values are smaller than for the model cluster Pt_{18}, but the values for a four-layer slab (0.12–0.13 eV) compare well with the result obtained with the cluster Pt_{52}. The

Table 3
Calculated structural and energetic properties of CO adsorbed on Pt(1 1 1) represented by the periodic model

θ/ML	Functional	Layers	Site	d_{C-S} (Å)	d_{C-O} (Å)	BE (eV)	ΔE (eV)
0.33	PW91	4	top	1.878	1.156	1.38	
				(1.856)	(1.158)	(1.51)	−0.14
			fcc	1.402	1.188	1.51	(−0.15)
				(1.371)	(1.190)	(1.66)	
		6	top	1.877	1.157	1.44	−0.14
			fcc	1.402	1.189	1.58	
		8	top	1.874	1.153	1.46	−0.12
			fcc	1.403	1.188	1.58	
	BP86	4	top	1.878	1.156	1.24	−0.10
			fcc	1.402	1.188	1.34	
0.11	PW91	4	top	1.878	1.155	1.40	−0.12
			fcc	1.400	1.190	1.52	

A coverage (θ) of 0.33 ML accounts for a $(\sqrt{3}\times\sqrt{3})$-R30° supercell, a coverage of 0.11 ML for a (3×3) supercell. The number of layers forming the slab is also provided. Data in parenthesis corresponds to results obtained with the same type of calculation, allowing the two uppermost layers to relax. See Table 1 for the definition of the specified values.

number of layers of the slab model has a small influence on this energy difference (Table 3), and roughly six layer thick slabs are required for a converged value. Surface relaxation stabilizes both adsorption modes in the same way, and hence it does not affect the energy difference. With another GGA functional (BP86), a weaker adsorption energy is calculated for both sites, comparable to the findings for the cluster models. The decrease of the coverage of CO from 1/3 to 1/9 ML stabilizes the adsorption at both sites by 0.1 eV, with no change in the energy difference between them. The low coverage calculation is the one that can be best compared with the cluster calculations, and the agreement with the Pt_{52} model is very good.

Calculated equilibrium geometries are very similar, with no significant changes due to either the model or the method (Table 3); they closely resemble the structure obtained with periodic calculations for the Pt_{52} cluster. This similarity is not surprising because the methodology is the very same. Moreover, for on top adsorption the agreement with LEED results is very good. It is indeed already known [74] that the convergence of the adsorption geometry is rather fast both with cluster size and slab thickness and that the xc functional employed has only a limited influence.

Unfortunately, the convergence of the total energy is more difficult. Energies depend strongly on the size of the cluster and, to a lesser extent, on the thickness of the slab model. Nevertheless, from our calculations, two general trends can be identified for the energy difference between the on top and the hollow site. On the one hand, the GGA functionals tend to favour the hollow site more than the hybrid B3LYP approach; for the Pt_{18} model, the energy difference is reduced by 0.27 eV with B3LYP (Table 1). On the other hand, the medium size Pt_{18} cluster ($\Delta E = -0.35$ eV; Table 1) tends to favour hollow site adsorption more than the large cluster Pt_{52} ($\Delta E = -0.15$ eV) or the slab models do.

Therefore, one may speculate that the correct on top adsorption structure would be favoured if the B3LYP functional were used on large clusters or on a slab model. Unfortunately, such a calculation is not feasible with the computer codes available to us. Nevertheless, extrapolation of known values could provide some estimates. If one corrects the Pt_{18} B3LYP result for the "cluster size effect" (0.2 eV, i.e. the difference between slab and cluster for Pt_{18}), the on top site is favered by 0.15 eV. Conversely, the Pt_{52} or slab GGA values can be corrected for the "hybrid functional effect" (0.27 eV, i.e. the difference between PW91 and B3LYP for Pt_{18}, Table 1), also favouring the top site by 0.1–0.15 eV. It is satisfactory that the two types of estimates are similar. Hence our calculations strongly indicate that the deficiency of GGA functionals for CO adsorption on Pt(1 1 1) could be rectified by choosing a hybrid functional like B3LYP in a slab model or in a large cluster calculation.

At this point, it is interesting to comment the work of Grinberg et al. [43]. They considered the results of Feibelman et al. [24] and suggested a general explanation for the DFT errors in binding energy differences attributing the failure of GGA for the site preference to the fact that bonds of different order are described with different accuracy. For the results of Kurth et al. [75], they showed that atomisation energy differences between bonds of different bond order, e.g. CO and NO, are poorly described, single bonds being always better described than multiple bonds. In the case of CO on Pt(1 1 1) they concluded that the CO bond is responsible for the error, because of the large bond order change in the hollow site with respect the atop one. Moreover, they suggest that a functional of superior performance in calculating atomisation energies might predict the right site preference. Hence, it seems appropriate to go one step further in that direction by analysing the CO bond in more detail.

4. Analysis of the bond

As indicated, GGA calculations favour adsorption of CO on Pt(1 1 1) at the hollow site. For the hybrid B3LYP approach, this preference is maintained but considerably reduced. Thus, it seems useful to analyse the bonding interaction between CO and the metallic surface and to discuss how this bond is affected by various xc functionals and cluster versus periodic calculations. As first step,

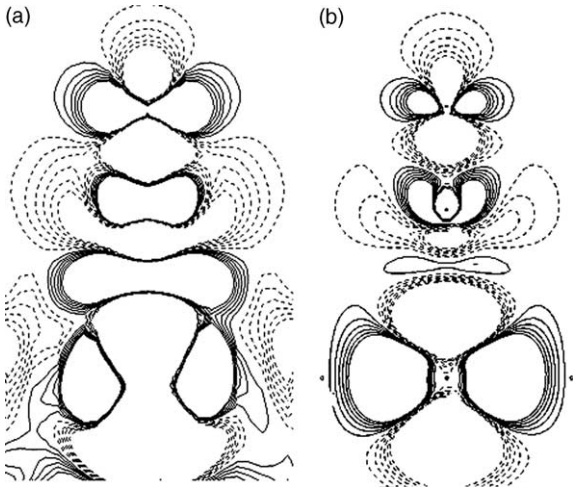

Fig. 3. Electron density difference maps between CO chemisorbed on top at Pt(1 1 1) and the separated fragments computed with the PW91 functional, for (a) plane wave basis set (four layers slab) and (b) localized basis set (Pt_{18} cluster model). Solid contours represent zones with accumulated electron density, and dashed contours are associated with zones of depleted electron density.

we compare electron density difference maps (Fig. 3) that can be interpreted using the simple model of Blyholder [76]; we do not attempt to compare with more detailed descriptions [77–80]. The cluster and the periodic approach lead to similar electronic redistributions upon adsorption with only small differences between the maps that can be attributed to the different basis sets used to represent the Kohn–Sham orbitals. The more localized features observed for cluster models are typical of local basis functions. In contrast, periodic models use plane waves that lead to more extended features in the difference map. The electronic redistribution occurring upon adsorption has been also monitored via the changes in the electronic population of CO molecular orbitals, calculated with the orbital projection technique [81] on the Pt_{18} cluster model (Table 4). As expected, the results are consistent with a larger donation and backdonation for the more coordinated hollow site.

The study of local density of states (LDOS) can also yield interesting information. Fig. 4a and b show LDOS curves of the CO chemisorbed system, for on top and fcc hollow sites respectively, obtained by projecting the wavefunction onto spherical harmonics centered at the position of the carbon and oxygen atoms.

According to the Blyholder model, the most interesting orbitals are 5σ and 2π; note, however, the participation of 4σ and 1π orbitals, which was manifested experimentally and described theoretically in Ref. [77,78] for CO on Cu and Ni surfaces. In the case of the on top site, the 5σ MO is more stabilized than in the fcc site, suggesting a stronger interaction with the metallic states. Moreover, because that peak is less intense in the fcc system, it can be deduced that less electron density exists in the 5σ state. This agrees with the decrease of the 5σ orbital population observed for cluster models, where a donation of 0.57 and 0.76 e, calculated with the B3LYP functional (Table 4) was found for on top and fcc sites, respectively. We will focus now on the energy range between -5 eV and the Fermi level; this interval is surprisingly vacant of $2p_x$ contributions of carbon, which can be rationalized as follows. Upon CO adsorption, there is significant mixing of the adsorbate 1π and 2π orbitals (the latter accounting for backdonation) with the metal d-band, generating three new hybrid π orbitals in an allylic configuration [77,78]. With such a picture of the bond, a new band is formed by an antibonding 1π and a bonding 2π admixture to the platinum d-band, leading to a

Table 4
CO molecular orbital population for CO chemisorbed at on top and hollow fcc sites, calculated by means of the orbital projection technique using the Pt_{18}–CO cluster model

Functional	Site	1σ	2σ	3σ	4σ	1π	5σ	2π
B3LYP	top	2.00	2.00	2.00	2.00	3.99	1.43	0.61
	fcc	2.00	2.00	2.00	1.99	3.97	1.24	1.05
PW91-HF	top	2.00	2.00	2.00	1.99	3.99	1.40	0.66
	fcc	2.00	2.00	2.00	1.99	3.96	1.22	1.09

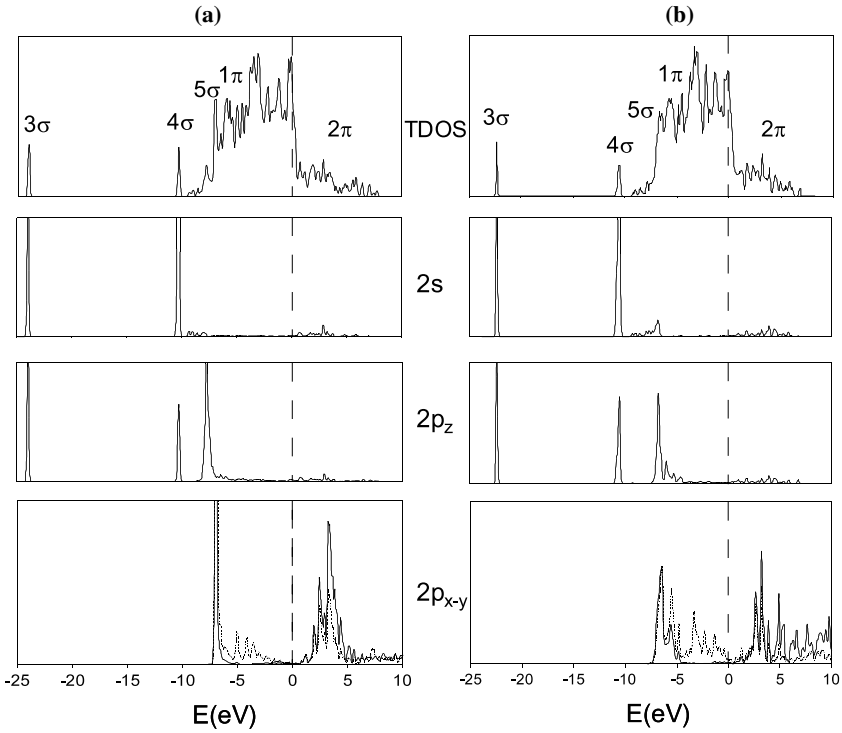

Fig. 4. Density of states for CO chemisorbed on Pt(1 1 1) computed using a plane wave basis set and the PW91 functional for the four layers slab system. Total LDOS and projections onto C_{2s}, C_{2pz}, C_{2px} and O_{2px} (dashed lines) atomic orbitals for on top (a) and fcc (b) adsorption sites.

cancellation of orbital amplitude at the carbon atom and an enforcement at the oxygen atom. This is consistent with the density of states depicted in Fig. 4 for the $2p_x$ projection, which shows a large participation of the oxygen atom. Comparing both adsorption sites, the integrated area of the peaks in that range of energies is larger for the hollow site, thus accounting for a higher backdonation. This is supported by the B3LYP calculated populations of 1.05 and 0.61 for fcc and on top sites, respectively (see Table 4), in good agreement with the accepted picture that the degree of backdonation increases with increasing coordination of CO [76–80].

To get a better understanding of the effect of the xc functional, we changed the amount of exact exchange included in the hybrid functional for the CO molecule, ranging from 0 (pure PW91) to 1 (only exact exchange); B3LYP corresponds to 0.2. Fig. 5 shows that the energies of the HOMO and

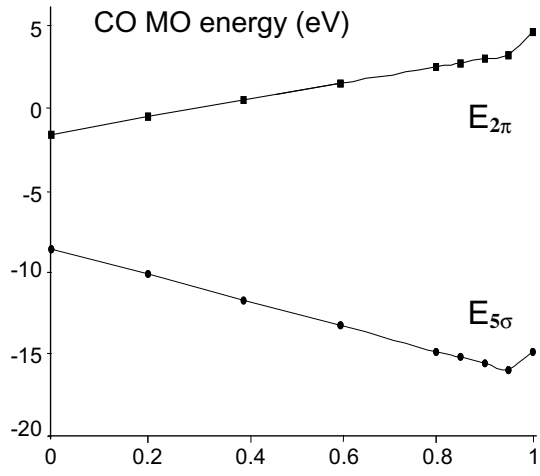

Fig. 5. HOMO (5σ) and LUMO (2π) energies of CO, as a function of the amount of exact exchange in a hybrid functional. The amount of the GGA exchange is reduced correspondingly.

LUMO of CO correlate in linear fashion with the percentage of exact exchange added to the functional. The main trend that can be deduced is that an increase of the exact exchange in the functional leads to an opening of the HOMO–LUMO gap [82–85]; the 5σ MO decreases in energy, and the 2π MO shifts upward. According to the Blyholder model, an opening in the HOMO–LUMO gap can account for a stabilization of the on top site compared with the fcc site, as explained in the following.

Previous analysis of the chemisorption of CO on Pt(1 1 1), based in the constrained space orbital variation (CSOV) technique, showed that π-backdonation is the most important contribution to the bond [23]. Therefore, a change in the modeling of this mechanism may have an important effect on the overall interaction. Calculations performed on the separated subsystems (CO and the cluster) showed notable differences in the electronic structure for different functionals. For the CO molecule, a PW91 calculation yields a LUMO energy of CO of about −2.1 eV, while a B3LYP calculation places the LUMO at −0.6 eV (see Scheme 1). On the other hand, both functionals furnish almost the same Fermi level for a platinum surface, about −5.4 eV, very close to the experimental work function of 5.7 eV. Therefore, when the adsorbate approaches the surface, backdonation from the metal d states to 2π CO MO is most favoured with the PW91 functional, because the energetic difference between the orbitals involved is smaller than in the case of B3LYP. This fact is also supported by the MO occupations calculated with both functionals (Table 4), showing a larger backdonation in the case of PW91 (the 2π orbital is more populated, by 0.04–0.05 e, than in the B3LYP description). Both donation and backdonation mechanisms are energetically favoured by the pure functional, a finding that also accounts for the higher binding energy found with this functional in comparison to the hybrid functional (see Tables 1 and 2). Thus, in the GGA description, with a smaller HOMO–LUMO gap, backdonation is more effective and the fcc site is stabilized with respect to the on top site. Inclusion of exact exchange reduces backdonation and preference for adsorption on fcc sites is reduced. Therefore, the xc functional has a large influence on the modeling of CO chemisorption processes at metal surfaces.

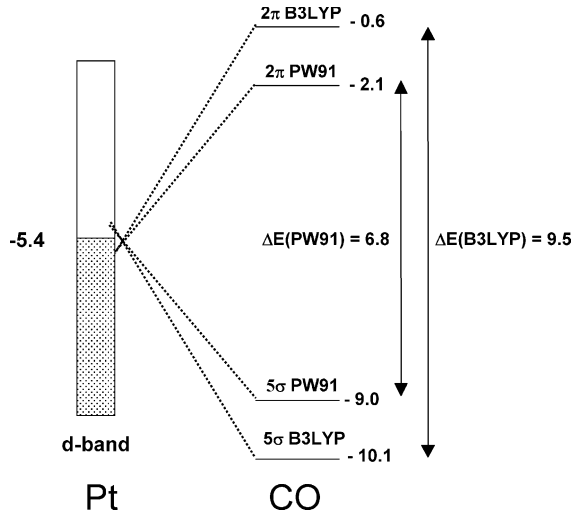

Scheme 1. Energies (eV) of 5σ and 2π CO molecular orbitals from B3LYP and PW91 calculations.

The comparison between top site and hollow site bonding has also been approached by two other recent studies. In one of them [43], the incorrect preference for hollow site adsorption was assigned to an underestimation of the CO internal bond energy loss upon adsorption on that site. In the other one [77,78], the intrinsic difficulty to balance adequately the contributions of σ and π states with an approximate functional was underlined. Our work goes beyond these aspects and points to the importance of including an exact exchange contribution in the energy functional for a better description of CO itself and its bonding with the Pt surface.

The experimental ionisation potential (IP) of CO is ∼14.1 eV [86]. In an exact Kohn–Sham description, this value would be reproduced by the negative of the HOMO energy [87,88]. Therefore, this value can be compared with the negative value of the HOMO energy for the CO molecule, −9.0 and −10.1 eV for PW91 and B3LYP methods, respectively. None of these functionals describes the value of that important property correctly, mainly because the Kohn–Sham potential derived from this functionals has a very poor asymptotic behaviour, leading to an artificial upward shift of

the one-electron energies of occupied orbitals [85]. On the other hand, the LUMO energy is a solution in exactly the same Kohn–Sham potential as the occupied orbitals; thus, it is not shifted upward as Hartree–Fock virtual orbitals. This fact accounts for the lower HOMO–LUMO gap showed by the PW91 orbitals, compared with B3LYP orbitals. A problem of current approximate xc functionals is that the exchange hole is too localized [85]; introducing a fraction of exact exchange renders the approximate hole somewhat more diffuse. In fact, this is the reason for the success of hybrid functionals [85–87]. However, the optimal amount of exact exchange may not be the same for all systems and situations.

5. Conclusions

In this work, a theoretical study of the chemisorption of carbon monoxide on Pt(1 1 1) surfaces is presented. Previous works (see [24] for a review) have shown that the two main methods used to study this system, namely cluster and periodic approaches, provide different results with regard to the site on which the CO molecule adsorbs on the platinum surface. A wide range of models and different techniques have been employed in those studies, however no conclusion was achieved to rationalize the cause of such disagreement. Therefore, in the present study, a series of density functional calculations was made, keeping the conditions for the cluster and periodic calculations as similar as possible. Employing the periodic approach, not only slab models, but also cluster models were used in order to compare directly with the localized basis set cluster calculations. Cluster models of good quality were chosen, with a correct description of all atoms involved in the adsorption process and also their first neighbors. The results of these calculations confirm the conjecture of Ref. [24] that both periodic and cluster methods provide the same energetic trend for the difference between the two adsorption sites studied, on top and threefold hollow. Our results also show that a good choice of the cluster is critical when accurate energetic results are required.

Although all models were good enough to provide a reasonable description of the structure of the system, all theoretical results fail to predict the experimental preference of the adsorption site of CO on Pt(1 1 1). Density functional calculations favour adsorption at the threefold hollow site over the on top adsorption (Tables 1–3), at variance with the experimental result. This discrepancy in the relative stability of the two sites remains even when different functionals are used. The B3LYP functional renders the on top and fcc sites almost degenerate, whereas the GGA functionals show a pronounced tendency to favour fcc adsorption. We also compared slab and cluster models using the GGA-PW91 functional in both cases. For the Pt_{18} cluster, the stability of the threefold hollow site is overestimated by 0.2 eV compared to slab models; the energy difference between the on top and the fcc sites was calculated to be $\sim$0.3 eV for the cluster model and only $\sim$0.1 eV for slab models. Only when the size of the cluster is significantly increased (e.g. in the model Pt_{52}), the energy difference between both sites is reduced (Table 3), approaching the value obtained with the slab model. Hence, the disagreement between slab and cluster models, found in the literature disappears with a well-chosen cluster model, large enough to overcome the known cluster size dependence of the total energy [40].

Comparing the two different GTO methods and the plane wave approach for clusters (Table 1), we note that the B3LYP functional predicts the two adsorption sites almost isoenergetic. For the same Pt_{18} cluster model the energy difference between the two sites is $\sim$0.3 eV when the PW91 functional is used in the slab model approach, which clearly favours adsorption at the fcc site. From a detailed comparative analysis of the various model results, we estimated that a slab model calculation, if performed with a hybrid B3LYP functional, should favour on top adsorption by $\sim$0.2 eV, in agreement with experiment.

An analysis of the electronic structure of the CO molecule obtained with different xc functionals showed that the ionisation potential is not well described with the PW91 functional. As a consequence, pertinent adsorbate levels are not placed properly relative to the Fermi level of the substrate

and, in turn, the donation-backdonation bonding mechanism is not adequately described with this functional. The PW91 functional puts occupied adsorbate energy levels closer to the Fermi level of the metal than the hybrid B3LYP functional. Therefore, the adsorbate interaction with the d-states of the platinum surface is stronger, both for donation and backdonation, and the adsorption energy at high coordination sites is overestimated with the PW91 functional.

The hybrid B3LYP functional yields the valence states of CO in closer agreement with experiment than GGA functionals, thus resulting in a better description of the chemisorption bond.

The present work hence gives a clear example of the usefulness of including exact exchange in the functional for cluster-size converged calculations when DFT is applied to chemisorption at metal surfaces.

Acknowledgements

A.G. acknowledges financial support through the TMR activity "Marie Curie research training grants" Grant no. HPMT-CT-2000-00166. JMR and NR are grateful for support from the exchange program Acciones Integradas/DAAD (HA2002-0001). NR acknowledges support from Deutsche Forschungsgemeinschaft and Fonds der Chemischen Industrie. Fundings from the Spanish Ministerio de Ciencia y Tecnología (BQU2002-04029-CO2-02) and the Catalan Government (2001SGR00315) are also acknowledged. A.G. and P.S. thank IDRIS (project 609) and CINES (project IRC2151) for generous allocation of CPU time.

References

[1] G.A. Somorjai, Introduction to Surface Chemistry and Catalysis, John Wiley & Sons Inc, New York, 1994, Chapter 7.8.2.
[2] M.E. Dry, Catal. Today 71 (2002) 227.
[3] Y.Y. Yeo, L. Vattuone, D.A. King, J. Chem. Phys. 106 (1997) 392.
[4] G.F. Cabeza, P. Légaré, N.J. Castellani, Surf. Sci. 465 (2000) 286.
[5] R.M. Watwe, B.E. Spiewak, R.D. Cortright, J.A. Dumesic, Catal. Lett. 51 (1998) 139.
[6] U. Engström, R. Ryberg, J. Chem. Phys. 112 (2000) 1959.
[7] B.H. Choi, A.P. Graham, K.T. Tang, J.P. Toennies, J. Chem. Phys. 112 (2000) 10538.
[8] A.P. Graham, J.P. Toennies, Europhys. Lett. 42 (1998) 449.
[9] N.M. Marković, T.J. Schmidt, B.N. Grgur, H.A. Gasteiger, R.J.. Behm, P.N. Ross, J. Phys. Chem. B 103 (1999) 8568.
[10] W.D. Mieher, L.J. Whitman, W. Ho, J. Chem. Phys. 91 (1989) 3228.
[11] J.V. Nekrylova, C. French, A.N. Artsyukhovich, V.A. Ukraintsev, I. Harrison, Surf. Sci. Lett. 295 (1993) L987.
[12] V.J. Kwasniewski, L.D. Schmidt, Surf. Sci. 274 (1992) 329.
[13] J. Liu, M. Xu, T. Nordmeyer, F. Zaera, J. Phys. Chem. 99 (1995) 6167.
[14] D.F. Ogletree, M.A. van Hove, G.A. Somorjai, Surf. Sci. 173 (1986) 351.
[15] K. Bleakley, P. Hu, J. Am. Chem. Soc. 121 (1999) 7644.
[16] A. Alavi, P. Hu, T. Deutsch, P.L. Silvestrelli, J. Hutter, Phys. Rev. Lett. 80 (1998) 3650.
[17] D. Curulla, A. Clotet, J.M. Ricart, F. Illas, J. Phys. Chem. 103 (1999) 5246.
[18] M. Lynch, P. Hu, Surf. Sci. 458 (2000) 1.
[19] H. Aizawa, S. Tsuneyuki, Surf. Sci. Lett. 399 (1998) L364.
[20] S. Ohnishi, N. Watari, Phys. Rev. B 49 (1994) 14619.
[21] C. Bureau, Chem. Phys. Lett. 269 (1997) 378.
[22] P.H.T. Philipsen, E. van Lenthe, J.G. Snijders, E.J. Baerends, Phys. Rev. B 56 (1997) 13556.
[23] F. Illas, S. Zurita, J. Rubio, A.M. Márquez, Phys. Rev. B 52 (1995) 12372.
[24] P.J. Feibelman, B. Hammer, J.K. Nørskov, F. Wagner, M. Scheffler, R. Stumpf, R. Watwe, J. Dumesic, J. Phys. Chem. B 105 (2001) 4018.
[25] H. Froitzheim, H. Hopster, H. Ibach, S. Lëhwald, Appl. Phys. 13 (1977) 147.
[26] H. Hopster, H. Ibach, Surf. Sci. 77 (1978) 109.
[27] H. Steininger, S. Lehwald, H. Ibach, Surf. Sci. 123 (1982) 264.
[28] G.S. Blackman, M.-L. Xu, D.F. Ogletree, M.A. van Hove, G.A. Somorjai, Phys. Rev. Lett. 61 (1988) 2352.
[29] J.A. Stroscio, D.M. Eigler, Science 254 (1991) 1319.
[30] P. Zeppenfeld, C.P. Lutz, D.M. Eigler, Ultramicroscopy 42–44 (1992) 128.
[31] M.Ø. Pedersen, M.-L. Bocquet, P. Sautet, E. Lægsgaard, I. Stensgaard, F. Besenbacher, Chem. Phys. Lett. 299 (1999) 403.
[32] M.-L. Bocquet, P. Sautet, Surf. Sci. 360 (1996) 128.
[33] R. Brako, D. Šokčević, Surf. Sci. 401 (1998) L388.
[34] C.F. Zinola, C. Gomis-Bas, G.L. Estiú, E.A. Castro, A.J. Arvia, Langmuir 14 (1998) 3901.
[35] A.B. Anderson, M.K. Awad, J. Am. Chem. Soc. 107 (1985) 7854.
[36] W.V. Glassey, R. Hoffmann, Surf. Sci. 475 (2001) 47.
[37] N.K. Ray, A.B. Anderson, Surf. Sci. 119 (1982) 35.

[38] K.A. Fichthorn, E. Gulari, R.M. Ziff, Surf. Sci. 243 (1991) 273.
[39] L. Wang, Q. Ge, G.D. Billing, Surf. Sci. Lett. 304 (1994) L413.
[40] I.V. Yudanov, R. Sahnoun, K.M. Neyman, N. Rösch, J. Chem. Phys. 117 (2002) 9887.
[41] J.P. Perdew, Y. Wang, Phys. Rev. B 45 (1992) 13244.
[42] J.P. Perdew, J.A. Chevary, S.H. Vosko, K.A. Jackson, M.R. Pederson, D.J. Singh, C. Fiolhais, Phys. Rev. B 46 (1992) 6671.
[43] I. Grinberg, Y. Yourdshahyan, A.M. Rappe, J. Chem. Phys. 117 (2002) 2264.
[44] M.-S. Liao, C.R. Cabrera, Y. Ishikawa, Surf. Sci. 445 (2000) 267.
[45] A.D. Becke, Phys. Rev. A 38 (1988) 3098.
[46] S.H. Vosko, L. Wilk, M. Nusair, Can. J. Phys. 58 (1980) 1200.
[47] J.P. Perdew, Y. Wang, Phys. Rev. B 33 (1986) 8800.
[48] S.A. Wasilesky, M.J. Weaver, M.T.M. Koper, J. Electroanal. Chem. 500 (2001) 344.
[49] F. Illas, F. Mele, D. Curulla, A. Clotet, J.M. Ricart, Electrochim. Acta 44 (1998) 1213.
[50] J.N. Miller, D.T. Ling, I. Lindau, P.M. Stefan, W.E. Spicer, Phys. Rev. Lett. 38 (1977) 1419.
[51] G. Ertl, M. Neumann, K.M. Streit, Surf. Sci. 64 (1977) 393.
[52] D.H. Winicur, J. Hurst, C.A. Becker, L. Wharton, Surf. Sci. 109 (1981) 263.
[53] M.T.M. Koper, R.A. van Santen, J. Electroanal. Chem. 476 (1999) 64.
[54] A.D. Becke, J. Chem. Phys. 98 (1993) 5648.
[55] M.J. Frisch et al., Gaussian 98, Revision A.7, Gaussian Inc, Pittsburgh, PA, 1998.
[56] P.J. Hay, W.R. Wadt, J. Chem. Phys. 82 (1985) 299.
[57] S.F. Boys, F. Bernardi, Mol. Phys. 19 (1970) 553.
[58] B.I. Dunlap, N. Rösch, Adv. Quantum Chem. 21 (1990) 317.
[59] Th. Belling, T. Grauschopf, S. Krüger, M. Mayer, F. Nörtemann, M. Staufer, C. Zenger, N. Rösch, in: H.-J. Bungartz, F. Durst, C. Zenger (Eds.), High Performance Scientific and Engineering Computing; Lecture in Computational Science and Engineering, vol. 8, Springer, Heidelberg, 1999, p. 439.
[60] Th. Belling, T. Grauschopf, S. Krüger, F. Nörtemann, M. Staufer, M. Mayer, V.A. Nasluzov, U. Birkenheuer, A. Shor, A. Matveev, A. Hu, N. Rösch, PARAGAUSS, Version 2.1, 1999; Technische Universität München.
[61] A.M. Ferrari, K.N. Neymann, T. Belling, M. Mayer, N. Rösch, J. Phys. Chem. B 103 (1999) 216.
[62] M. García-Hernández, U. Birkenheuer, A. Hu, F. Illas, N. Rösch, Surf. Sci. 471 (2001) 151.
[63] N. Rösch, S. Krüger, M. Mayer, V.A. Nasluzov, in: J.M. Seminario (Ed.), Recent Developments and Applications of Modern Density Functional Theory, Elsevier, Amsterdam, 1996, p. 497.
[64] B. Hammer, L.B. Hansen, J.K. Nørskov, Phys. Rev. B 59 (1999) 7413.
[65] G. Kresse, J. Hafner, Phys. Rev. B 47 (1993) 558.
[66] G. Kresse, J. Hafner, Phys. Rev. B 48 (1993) 13115.
[67] G. Kresse, J. Hafner, Phys. Rev. B 49 (1994) 14251.
[68] G. Kresse, J. Joubert, Phys. Rev. B 59 (1999) 1758.
[69] H.J. Monkhorst, J.D. Pack, Phys. Rev. B 13 (1976) 5188.
[70] A. Görling, S.B. Trickey, P. Gisdakis, N. Rösch, in: J. Brown, P. Hofmann (Eds.), Topics in Organometallic Chemistry, vol. 4, Springer, Heidelberg, 1999, p. 109.
[71] A. Matveev, M. Staufer, M. Mayer, N. Rösch, Int. J. Quantum Chem. 75 (1999) 863.
[72] I. Panas, J. Schüle, P.E.M. Siegbahn, U. Wahlgren, Chem. Phys. Lett. 149 (1988) 265.
[73] P.E.M. Siegbahn, L.G.M. Pettersson, U. Wahlgren, J. Chem. Phys. 94 (1991) 4024.
[74] G. Pacchioni, Heterogeneous Chem. Rev. 2 (1995) 213.
[75] S. Kurth, J.P. Perdew, P. Blaha, Int. J. Quantum Chem. 75 (1999) 889.
[76] G. Blyholder, J. Phys. Chem. 68 (1964) 2772.
[77] A. Föhlisch, M. Nyberg, J. Hasselström, O. Karis, L.G.M. Pettersson, A. Nilsson, Phys. Rev. Lett. 85 (2000) 3309.
[78] A. Föhlisch, M. Nyberg, P. Bennich, L. Triguero, J. Hasselström, O. Karis, L.G.M. Pettersson, A. Nilsson, J. Chem. Phys. 112 (2000) 1946.
[79] M. Staufer, U. Birkenheuer, T. Belling, F. Nörtemann, N. Rösch, M. Stichler, C. Keller, W. Wurth, D. Menzel, L.G.M. Pettersson, A. Föhlisch, A. Nilsson, J. Chem. Phys. 111 (1999) 4704.
[80] F. Ample, D. Curulla, F. Fuster, A. Clotet, J.M. Ricart, Surf. Sci. 497 (2002) 154.
[81] P.S. Bagus, F. Illas, Phys. Rev. B 42 (1990) 10852.
[82] J. Muscat, A. Wander, N.M. Harrison, Chem. Phys. Lett. 342 (2001) 397.
[83] M. Albrecht, P. Fulde, H. Stoll, Chem. Phys. Lett. 319 (2000) 355.
[84] I.P.R. Moreira, F. Illas, R.L. Martin, Phys. Rev. B 65 (2002) 155102.
[85] E.J. Baerends, O.V. Gritsenko, J. Phys. Chem. A 101 (1997) 5383.
[86] P. Erman, A. Karawajczyk, E. Rachlew-Kallne, C. Stromholm, J. Larsson, A. Persson, R. Zerne, Chem. Phys. Lett. 215 (1993) 173.
[87] J.P. Perdew, R.G. Parr, M. Levy, J.L. Balduz, Phys. Rev. Lett 49 (1982) 191.
[88] W. Koch, M.C. Holthausen, A Chemist's Guide to Density Functional Theory, Wiley, Weinheim, 2001.